Phytochemistry 164 (2019) 67–77

Contents lists available at ScienceDirect

Phytochemistry

journal homepage: www.elsevier.com/locate/phytochem

Cytotoxic saponins and other natural products from flowering tops of *Narthecium ossifragum* L

Andrea Estefanía Carpinteyro Díaz[a], Lars Herfindal[b], Bendik Auran Rathe[b], Kristine Yttersian Sletta[b], Anni Vedeler[c], Svein Haavik[b], Torgils Fossen[a,*]

[a] Department of Chemistry and Centre for Pharmacy, University of Bergen, Allégt. 41, N-5007 Bergen, Norway
[b] Department of Clinical Science and Centre for Pharmacy, University of Bergen, Norway
[c] Department of Biomedicine, University of Bergen, Norway

ARTICLE INFO

Keywords:
Narthecium ossifragum (L.) huds
Nartheciaceae
Flowers
Cytotoxicity
Toxicity
Saponins
di-C-Glycosylflavones
2D NMR

ABSTRACT

For more than four centuries, the intake of *Narthecium ossifragum* has been associated with poisoning in domesticated animals. Saponins occurring in flowering tops of the plant are considered to cause kidney damage in calves. At present, there are more than 30 papers on the saponins of *N. ossifragum* in the literature, although the structures of these compounds have hitherto not been determined. Here, we identify the saponins of *N. ossifragum* as sarsasapogenin, sarsasapogenin-3-*O*-*β*-galactopyranoside, sarsasapogenin-3-*O*-(2′-*O*-*β*-glucopyranosyl-*β*-galactopyranoside) and sarsasapogenin-3-*O*-(2′-*O*-*β*-glucopyranosyl-3′-*O*-*α*-arabinopyranosyl-*β*-galactopyranoside). Moreover, six aromatic natural products were isolated and characterized from the methanolic extract from flowers of *N. ossifragum*. Five of these aromatic compounds, chrysoeriol 6-*C*-*β*-arabinofuranoside-8-*C*-*β*-glucopyranoside, chrysoeriol 6-*C*-*β*-arabinopyranosyl-8-*C*-*β*-glucopyranoside, chrysoeriol 6-*C*-*β*-xylopyranosyl-8-*C*-*β*-galactopyranoside, chrysoeriol 6-*C*-*β*-galactopyranosyl-8-*C*-*β*-glucopyranoside and chrysoeriol 6-*C*-*β*-glucopyranosyl-8-*C*-*β*-galactopyranoside are undescribed. All compounds were tested for cytotoxicity in mammalian cell lines derived from the heart, kidney, and haematological tissues. The saponins exhibited cytotoxicity in the micromolar range, with proportionally increasing cytotoxicity with increasing number of glycosyl substituents. The most potent compound was the main saponin sarsasapogenin-3-*O*-(2′-*O*-*β*-glucopyranosyl-3′-*O*-*α*-arabinopyranosyl-*β*-galactopyranoside), which produced cell death at concentrations below 3–4 μM in all three cell lines tested. This indicates that the saponins are the toxicants mainly responsible for kidney damage observed in cattle after ingestion of *N. ossifragum*. Our findings also pave the way for analysis of individual compounds isolated during the biopsies of intoxicated animals.

1. Introduction

Narthecium ossifragum (L.) Huds. (Nartheciaceae) is a perennial flowering plant (Fig. 1), which natively grows on bogs in western and north-western Europe. Flowering of this species occurs between July and August (Mossberg et al., 1995). The bright yellow flowers are 10–16 mm wide and occur in clusters with 6–20 flowers (Feilberg, 1999). The first available information about the potential toxicity of this plant was published in 1667 by the physician and botanist Simon Paulli in what is known to be the first Norwegian scientific publication (Paulli, 1667). The plant has in several instances been associated with toxic effects in grazing animals (Stabursvik, 1953; Flåøyen et al., 1995a; Wisløff et al., 2003) and is considered to cause the phototoxic disease alveld in lambs (Stabursvik, 1953). This livestock poisoning is both economically important and an animal welfare problem especially in the Nordic countries (Bernhoft, 2010). It has been suggested that alveld may be caused by metabolite(s) produced by *N. ossifragum* (Abdelkader et al., 1984), an associated fungus (di Menna et al., 1992) or cyanobacteria (Tønnesen et al., 2013). However, an explanation for the observed toxic effects associated with intake of *N. ossifragum* at the molecular level has not been provided in the current literature.

In numerous publications, the flowering tops of *N. ossifragum* have been reported to contain significant amounts of saponins, which are considered to be toxic components of the plant (Uhlig et al., 2007). Saponins occurring in the flowering tops of the plant are presumed to cause kidney damage in calves (Flåøyen et al., 1997). These compounds have been suggested as playing a role in the development of hypothesized secondary phototoxicity although this view has been challenged

* Corresponding author. .
E-mail address: Torgils.Fossen@uib.no (T. Fossen).

https://doi.org/10.1016/j.phytochem.2019.04.014
Received 18 January 2019; Received in revised form 17 April 2019; Accepted 24 April 2019

Fig. 1. Flowers of *N. ossifragum*. Photo: Andrea Estefanía Carpinteyro Díaz.

(Flåøyen et al., 1991). Even though more than thirty publications in the current literature deal with saponins of *N. ossifragum*, none of these compounds has hitherto been characterized in detail from this plant source and their molecular structures remain unknown. Stabursvik (1959) identified the aglycone of the saponins of *N. ossifragum* to be sarsasapogenin (Stabursvik, 1959). Ceh and Hauge (1981) tentatively identified two saponins from *N. ossifragum* based on sarsasapogenin (spirostan-3-ol) aglycone. Both of these saponins were indicated to be glycosylated with trisaccharides consisting of galactose-glucose-arabinose (major compound) and galactose-glucose-xylose (minor compound), respectively, where the trisaccharide moiety was attached at C-3 of the aglycone. The names narthecin and xylosin were suggested for these saponins. However, the linkages between the individual sugar units were not determined (Ceh and Hauge, 1981) and the structures were not confirmed by NMR spectroscopy and HR-MS. Using LC-MS Uhlig et al. (2007) tentatively identified saponins based on smilagenin and sarsasapogenin with two and three sugar units. However, neither the sugar composition nor the individual glycosyl substituents could be identified (Uhlig et al., 2007). Even though the connection between the intake of *N. ossifragum* and the occurrence of alveld in lambs seems to be well documented (Abdelkader et al., 1984; Ceh and Hauge, 1981) the original assumption about a potential connection between saponins of this plant species and the phototoxic disease is controversial and has been challenged (Flåøyen et al., 1991). Abdelkader et al. (1984) reported that lambs fed with a crude mixture of saponins developed alveld. However, the same authors reported that the most purified fraction of saponins did not induce alveld in lambs. Moreover, Flåøyen et al. (1991) reported that lambs fed with large quantities of freeze-dried *N. ossifragum*, containing significant amounts of saponins, did not develop alveld. Surprisingly, the possibility that alveld may be caused by aromatic compounds unique to *N. ossifragum* with the ability to fluoresce has not been considered in current literature. Further progress in research into the potential structure-activity role of the saponins of *N. ossifragum* in connection with their potential role as nephrotoxins poisoning cattle is severely hampered by the fact that their structures have not yet been determined and the lack of methodology for large-scale isolation of these compounds.

In this paper we report on structure determination and cytotoxicity of individual saponins of *N. ossifragum*. A methodology for large-scale separation and isolation of these compounds in the pure state is provided for the first time. Although the content of aromatic compounds of the fruits of *N. ossifragum* has been thoroughly characterized (Vu et al., 2016) no aromatic compound has hitherto been identified from the plant at the flowering stage, i.e. at the development stage where intake of *N. ossifragum* has been associated with lifestock toxicity. As part of our on-going research concerning the characterization of aromatic compounds from *N. ossifragum*, several di-*C*-glycosylflavones, including several previously undescribed compounds, were isolated for the first time from this plant source.

2. Results and discussion

The methanolic extracts of 1.7 kg of flowering tops of *N. ossifragum* were concentrated under reduced pressure and subjected to liquid/liquid separation with petroleum ether followed by ethyl acetate.

A total of 7.1546 g white precipitate was collected from the concentrated petroleum ether and ethyl acetate phases, corresponding to approximately 2.3% of the total dry weight of the plant material. The white precipitate was identified as a mixture of saponins by the recorded 1D and 2D NMR spectra, where glycosyl substituents attached to an aliphatic aglycone were observed. One gram of this mixture was further purified by Sephadex LH-20 column chromatography. Individual pure saponins were then isolated by silica column chromatography. The individual pure saponins were identified as sarsasapogenin (**1**), sarsasapogenin-3-*O*-*β*-galactopyranoside (**2**), sarsasapogenin-3-*O*-(2′-*O*-*β*-glucopyranosyl-*β*-galactopyranoside) (**3**) and sarsasapogenin-3-*O*-(2′-*O*-*β*-glucopyranosyl-3′-*O*-*α*-arabinopyranosyl-*β*-galactopyranoside) (**4**) by 1D and 2D NMR spectroscopy (Tables 2 and 3, Fig. 2 and Supplementary Figs. S1–S34) and high resolution mass spectrometry (Supplementary Figs. S70–72). The 1D ^{1}H NMR spectrum of compound **4** showed the presence of sarsasapogenin aglycone in addition to three glycosyl substituents (Figure S26) The glycosyl units were identified to be galactopyranosyl, glucopyranosyl and arabinopyranosyl by the 17 ^{13}C signals observed in the 1D^{13}C CAPT NMR spectrum of **4**. The ^{13}C signals belonging to these sugar units were in agreement with reference values of galactopyranosyl, glucopyranosyl and arabinopyranosyl, respectively (Inoue et al., 1995; Fossen and Andersen, 2006). The combined information in the 2D ^{1}H–^{1}H COSY spectrum and the 2D ^{1}H–^{13}C edited HSQC spectrum, the 2D ^{1}H–^{13}C HSQC-TOCSY spectrum and the 2D ^{1}H–^{13}C H2BC spectrum were of paramount importance with respect to complete assignments of all ^{1}H and ^{13}C resonances belonging to the glycosyl substituents (Figs. S28–S34 and Tables 1 and 2). The identities of the glycosyl substituents were further confirmed by the observed coupling constants in the 1D ^{1}H NMR spectrum and the 1D ^{1}H selective TOCSY spectra of **4** (Table 1). The configurations of C-1′, C-1″ and C-1‴ belonging to the galactopyranosyl, the glucopyranosyl and the arabinopyranosyl units, respectively, were determined to be in *β*-configuration for the former two units and in *α*-configuration for the latter, by the observed large $^{3}J_{HH}$ vicinal coupling constants of 7.7 Hz, 7.9 Hz and 7.2 Hz (Table 1). The configurations of the anomeric carbons were

Table 1
^{1}H NMR chemical shift values (ppm) and coupling constants (Hz) for saponins **1–4** isolated from flowering tops of *N. ossifragum* in DMSO-D_6 at 298K. s = singlet; d = doublet; dd = double doublet; dt = double triplet; p = pentet; m = multiplet.

	1	2	3	4
1A	1.37	1.40	1.41	1.48
1B	1.33	1.35	1.34	1.30
2A	1.38	1.51	1.55	1.48
2B	1.31	1.40	1.38	1.41
3	3.86 *m*	3.88 *m*	3.89 *m*	3.88 *m*
4A	1.81	1.71	1.71	1.67
4B	1.16	1.41	1.42	1.39
5	1.67	1.71	1.71	1.84
6A	1.81	1.79	1.78	1.76
6B	1.06	1.08	1.09	1.06
7A	1.35	1.36	1.35	1.34
7B	1.02	1.03	1.02	1.02
8	1.51	1.51	1.51	1.51
9	1.32	1.34	1.33	1.33
10				
11A	1.32	1.33	1.33	1.33
11B	1.17	1.18	1.17	1.14
12A	1.65	1.66	1.65	1.65
12B	1.12	1.13	1.12	1.12
14	1.13	1.14	1.14	1.14
15A	1.88	1.89	1.89	1.88
15B	1.13	1.13	1.13	1.13
16	4.26 *m*	4.27 *m*	4.27 *m*	4.27 *m*
17	1.65	1.65	1.65	1.65
18	0.69 *s*	0.70 *s*	0.70 *s*	0.70 *s*
19	0.89 *s*	0.90 *s*	0.89 *s*	0.89 *s*
20	1.75 *p* 6.8	1.75 *p* 6.8	1.75 *p* 6.5	1.75 *p* 6.9
21	0.92 *d* 7.0	0.92 *d* 7.0	0.92 *d* 7.0	0.92 *d* 7.0
22				
23A	1.88	1.88	1.88	1.88
23B	1.33	1.33	1.34	1.34
24A	1.79	1.79	1.79	1.79
24B	1.26	1.26	1.26	1.26
25	1.63	1.63	1.63	1.63
26A	3.77 dd 2.9, 11.0	3.77 dd 2.8, 11.0	3.78 dd 2.8, 11.1	3.78 dd 2.8, 11.0
26B	3.20 dt 11.0, 1.8	3.20 dt 11.0, 1.8	3.20 dt 1.7,11.1	3.20 dt 1.9, 11.4
27	1.00 *d* 7.1	1.00 *d* 7.1	1.00 *d* 7.1	1.00 *d* 7.1
3-OH	4.15 *d* 3.1			
3-*O*-*β*-Galactopyranoside				
1'		4.08 *d* 7.5Hz	4.24 *d* 5.9Hz	4.27 *d* 7.7
2'		3.24	3.57	3.75 dd 9.8, 7.7
3'		3.24	3.48	3.56 dd 3.1, 9.8Hz
4'		3.61	3.65	3.81 dd 3.1, 1.0
5'		3.27 dt 6.2, 1.0	3.30	3.34
6A'		3.50 dd 6.2, 11.0	3.50	3.48 dd 12.0, 6.1
6B'		3.40 dd 6.2, 11.0	3.40 *p* 5.6Hz	3.38 dd 12.0, 1.6
2′-*O*-*β*-Glucopyranosyl				
1''			4.39 *d* 7.9Hz	4.64 *d* 7.9
2''			2.97	2.86 dd 7.9, 9.0
3''			3.15	3.11 t 9.0
4''			3.11 *d* 4.6Hz	2.96 dd 9.6, 9.0
5''			3.03	3.07 ddd 9.6, 6.3, 2.7
6A''			3.62 *m*	3.68 dd 12.2, 2.7
6B''			3.49	3.43
3′-*O*-*α*-arabinopyranosyl				
1'''				4.41 *d* 7.2
2'''				3.42
3'''				3.28
4'''				3.62
5A'''				3.68
5B'''				3.38

Table 2
^{13}C NMR chemical shift values (ppm) for saponins **1–4** isolated from flowering tops of *N. ossifragum* in DMSO-D_6 at 298K.

	1	2	3	4
1	29.8	30.16	30.14	29.88
2	27.5	26.08	25.96	26.19
3	64.6	72.79	73.90	72.99
4	33.4	29.59	29.97	29.43
5	36.0	35.97	36.00	34.42
6	26.4	26.40	26.34	26.40
7	26.2	26.22	26.22	26.25
8	35.0	34.95	34.95	34.98
9	39.4	39.50	39.50	39.50
10	34.8	34.65	34.58	34.61
11	20.5	20.51	20.50	20.51
12	39.7	39.70	39.7	39.7
13	40.2	40.0	40.27	40.29
14	55.8	55.73	55.77	55.79
15	31.5	31.47	31.47	31.49
16	80.5	80.45	80.46	80.48
17	61.9	61.91	61.91	61.92
18	16.2	16.24	16.25	16.29
19	23.8	23.63	23.63	23.51
20	41.6	41.62	41.62	41.64
21	14.5	14.53	14.53	14.55
22	108.9	108.91	108.91	108.93
23	25.5	25.50	25.50	25.50
24	25.6	25.59	25.59	26.61
25	26.5	26.50	26.51	26.52
26	64.3	64.31	64.32	64.32
27	16.0	15.99	15.99	16.01
3-*O*-*β*-Galactopyranoside				
1'		101.83	100.81	99.83
2'		70.76	79.21	75.49
3'		73.65	73.27	82.10
4'		68.19	67.72	68.02
5'		75.05	74.78	74.62
6'		60.42	60.30	60.09
2′-*O*-*β*-Glucopyranosyl				
1''			103.90	102.20
2''			75.21	74.68
3''			76.22	76.79
4''			70.08	71.10
5''			77.02	76.65
6''			61.12	61.89
3′-*O*-*α*-arabinopyranosyl				
1'''				104.70
2'''				70.97
3'''				72.88
4'''				67.94
5'''				65.85

Table 3
UV data for compounds **5–10** isolated from flowering tops of *N. ossifragum*.

Compound	λ_{max} I	λ_{max} II
5	346	271
6	347	270
7	347	269
8	347	270
9	346	270
10	346	270

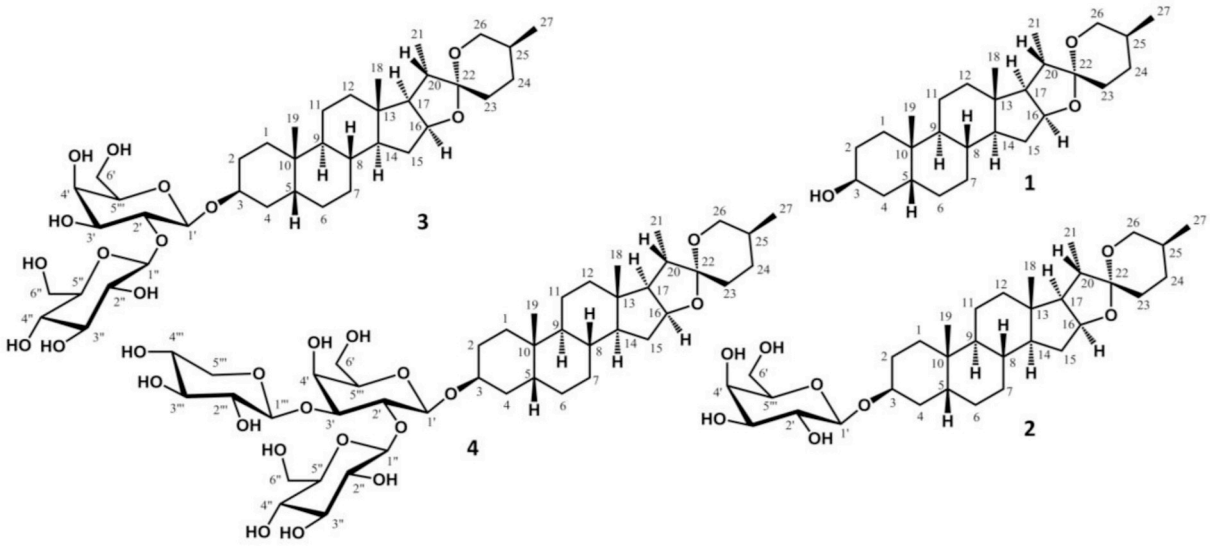

Fig. 2. Structures of sarsasapogenin (**1**), sarsasapogenin-3-O-*β*-galactopyranoside (**2**), sarsasapogenin-3-*O*-(2′-*O*-*β*-glucopyranosyl-*β*-galactopyranoside) (**3**) and sarsasapogenin-3-*O*-(2′-*O*-*β*-glucopyranosyl-3′-*O*-*α*-arabinopyranosyl-*β*-galactopyranoside) (**4**) isolated from flowering tops of *N. ossifragum*.

further confirmed by the $^{1}H–^{13}C$ coupling constants of H-1'/C-1' (163 Hz), H-1''/C-1'' (162 Hz) and H-1‴/C-1‴ (164 Hz), which are in agreement with literature values for *β*-galactopyranosyl, *β*-glucopyranosyl and *α*-arabinopyranosyl, respectively (Pedersen et al., 1995). The crosspeaks at δ 4.27/73.0 (H-1'/C-3), δ 3.88/99.8 (H-3/C-1′) observed in the HMBC spectrum and the crosspeaks at δ 4.27/3.88 (H-1'/H-3), δ 4.27/1.67 (H-1'/H-4A), δ 4.27/1.48 (H-1'/H-2A) and δ 4.27/1.39 (H-1'/H–4B) observed in the ROESY spectrum confirmed the linkage between the galactopyranosyl unit and the aglycone to be at the 3-position. The crosspeaks at δ 4.64/75.5 (H-1''/C-2′), δ 3.75/102.2 (H-2′/C-1″) observed in the HMBC spectrum and the crosspeak at δ 4.64/3.75 (H-1''/H-2′) observed in the ROESY spectrum confirmed the linkage between the glucopyranosyl and the galactopyranosyl units to be at the 2′-position. The crosspeaks at δ 4.41/82.1 (H-1‴/C-3′), δ 3.56/104.7 (H-3'/C-1‴) observed in the HMBC spectrum and the crosspeak at δ 4.41/3.56 (H-1‴/H-3′) observed in the ROESY spectrum confirmed the linkage between the arabinopyranosyl and the galactopyranosyl units to be at the 3′-position. Thus, **4**, which is the main saponin of *N. ossifragum*, was identified as sarsasapogenin-3-*O*-(2′-*O*-*β*-glucopyranosyl-3′-*O*-*α*-arabinopyranosyl-*β*-galactopyranoside). A sodiated molecular ion [MNa^{+}] at *m/z* 895.46624 (calculated: 895.46681; Mass difference: −0.53 ppm) observed in the high-resolution mass spectrum of **4** (Fig. S72) corresponding to $C_{27}H_{30}O_{15}Na$ confirmed this identity. Following a similar strategy, compounds **1**, **2** and **3** were identified as sarsasapogenin (**1**), sarsasapogenin-3-*O*-*β*-galactopyranoside (**2**) and sarsasapogenin-3-*O*-(2′-*O*-*β*-glucopyranosyl-*β*-galactopyranoside) (**3**), respectively.

The stereochemistry of the sapogenin aglycones of compounds **1**–**4** were determined to be (3β,5β,25R/S)-spirostan-3-ol by 2D ^{1}H ROESY NMR (Fig. 3); with the same stereochemistry as the aglycone sarsasapogenin reported in the literature (Inoue et al., 1995). Inoue et al. (1995) reported that compound **4**, which is also present in *N. asiaticum* occurred as a racemic mixture of compounds with R/S configurations of C25, respectively. The specific rotation of compound **4** isolated from *N. ossifragum* was −2.86°, indicating that compound **4** occur as a similar racemic mixture (Inoue et al., 1995). According to Li et al. (2013) L-glucose does not occur naturally in higher living organisms. The same applies to L-galactose (Li et al., 2013), whereas the prevalent L-arabinose is the structural equivalent to D-glucose (Gaffield et al., 1977).

Stabursvik (1959) indicated the presence of sarsasapogenin, as well as unidentified glycosylated derivatives thereof, in flowering tops of *N. ossifragum* (Stabursvik, 1959). Ceh and Hauge (1981) previously tentatively identified two saponins from *N. ossifragum* based on sarsasapogenin (spirostan-3-ol) aglycone. Without determining the linkages between the individual glycosyl units, these saponins were indicated to be glycosylated with trisaccharides consisting of galactose-glucose-arabinose (major compound) and galactose-glucose-xylose (minor compound), respectively, where the trisaccharide moiety was attached at C-3 of the aglycone (Ceh and Hauge, 1981). We identified sarsasapogenin-3-*O*-(2′-*O*-*β*-glucopyranosyl-3′-*O*-*α*-arabinopyranosyl-*β*-galactopyranoside) as the main saponin of *N. ossifragum*. This compound, in addition to sarsasapogenin-3-*O*-(2′-*O*-*β*-glucopyranosyl-*β*-galactopyranoside), has previously been identified in the related Asian species *N. asiaticum* (Inoue et al., 1995). Sarsasapogenin-3-*O*-*β*-galactopyranoside is identified for the first time in the genus Narthecium. The compound has previously been identified in *Anemarrhena asphodeloides* (Bge) (Sy et al., 2016).

Brine shrimp lethality assay is a simple *in vivo* test for the cytotoxicity of biochemicals (Wu, 2014) where the test organisms are *Artemia salina* nauplii (Harwig and Scott, 1971; Meyer et al., 1982). Initial toxicity tests indeed revealed that a mixture of the above described saponins of *N. ossifragum* proved to be potent toxins for *Artemia salina* nauplii with LC_{50} value of 8.7 μg/mL, which encouraged more extensive and through-depth studies of their cytotoxic potential, as described below.

The components of the aqueous phase were further separated by gradient XAD-7 adsorption chromatography, Sephadex LH-20 gel filtration chromatography and preparative HPLC. The UV spectra of compounds **5**–**10** recorded on-line during HPLC analysis (Table 3) showed UV maximum absorptions at 346–347 nm and 269–271 nm indicating that these compounds have a flavone core structure. These six compounds were identified by a combination of 1D and 2D NMR spectroscopic techniques and high resolution mass spectrometry, as described below. Compound **10** was identified as the known compound chrysoeriol 6,8-di-*C*-*β*-glucopyranoside (**10**) by a combination of 1D and 2D NMR spectroscopy and high-resolution mass spectrometry. A di-C-glycoside of chrysoeriol was first indicated to occur in the moss *Mnium affine* Bland (Melchert and Alston, 1965). Chrysoeriol 6,8-di-*C*-*β*-glucopyranoside was originally identified in *Larrea tridentata* (Sakakibara et al., 1977). The compound has also been identified in several quite diverse sources such as *Spergularia rubra* (Bouillant et al., 1979), the liverwort *Trichocolea tomentella* (Mues, 1982) and *Tricophorum cespitosum* (Salmenkallio et al., 1982).

The downfield region of the 1D ^{1}H NMR spectrum of compound **5**

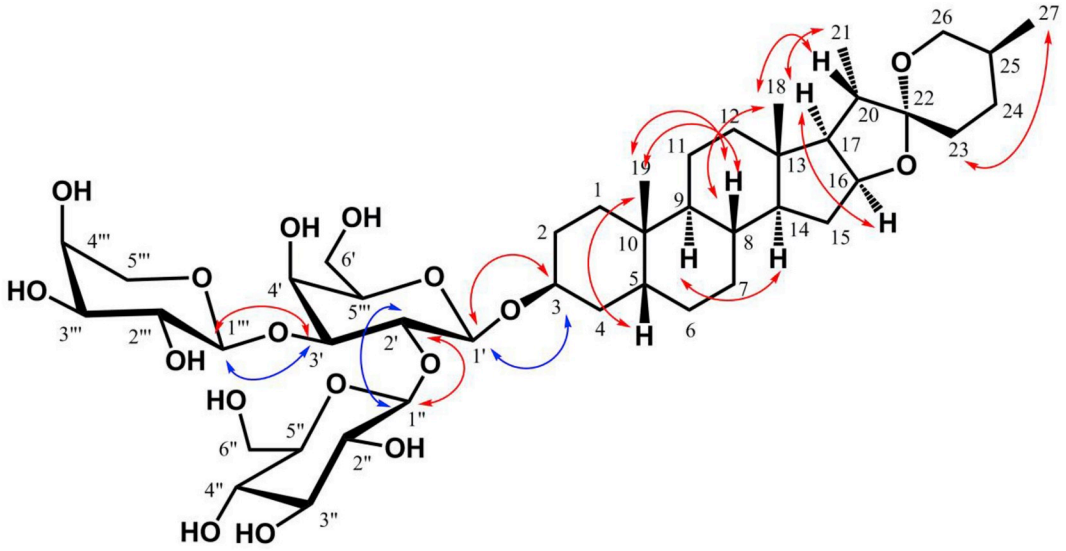

Fig. 3. HMBC correlations (blue curved arrows) and ROE correlations (red curved arrows) important for complete structure determination of sarsasapogenin-3-*O*-(2′-*O*-*β*-glucopyranosyl-3′-*O*-*α*-arabinopyranosyl-*β*-galactopyranoside) (**4**) isolated from flowering tops of *N. ossifragum*. (For interpretation of the references to colour in this figure legend, the reader is referred to the Web version of this article.)

showed a 3H ABX system at δ 7.55 (d 2.2 Hz; H-2′), δ 7.73 (dd 8.3, 2.2 Hz; H-6′) and δ 6.88 (d 8.3 Hz; H-5′), in addition to a 1H singlet at δ 6.94 (H-3), which is in accord with chrysoeriol aglycone with substituents at C-6 and C-8. A 3H signal corresponding to a methoxy group attached to the 3′-position of the aglycone of **5** was observed at δ 3.88 ppm. The methoxy group was confirmed to be attached to C-3′ of the aglycone by the crosspeak at δ 3.88/148.0 (3′-OCH_3/C-3′) observed in the HMBC spectrum of **5** and the crosspeak at δ 3.88/7.55 (3′-OCH_3/H-2′) observed in the ROESY spectrum of **5**. The glycosyl substituent attached to the 6-position of the aglycone was identified as arabinofuranose by the observed ^1H–^1H coupling constants in the 1D 1H NMR spectrum, in addition to the characteristic downfield shifts of C-2″, C-3″ and C-4″ of this glycosyl unit (Fossen and Andersen, 2006). The linkage between the arabinofuranosyl and chrysoeriol aglycone was confirmed to be at the 6-position by the observed crosspeaks at δ 5.44/162.7 (H-1″/C-7), δ 5.44/157.1 (H-1″/C-5) and δ 5.44/103.3 (H-1″/C-6) in the 2D ^1H–^{13}C HMBC spectrum of **5** (Fig. S38) and the crosspeak at δ 5.44/13.81 (H-1″/5-OH) observed in the 2D 1H ROESY spectrum of **5** (Fig. S41).

The glycosyl unit attached to the 8-position of the aglycone of **5** was identified as glucose by observation of seven proton resonances, where large axial-axial coupling constants between the ring protons of the glycosyl were found, and the characteristic values (Fossen and Andersen, 2006) of the six ^{13}C resonances belonging to this unit (Table 5). The anomeric coupling constant (9.9 Hz) observed in the 1D ^1H NMR spectrum of **5** confirmed the *β*-configuration of H-1‴. The linkage between the glucopyranosyl and chrysoeriol aglycone was confirmed to be at the 8-position by the observed crosspeaks at δ 4.70/162.7 (H-1‴/C-7), δ 4.70/154.9 (H-1‴/C-9) and δ 4.70/104.5 (H-1‴/C-8) in the 2D ^1H–^{13}C HMBC spectrum of **5** (Fig. S38). Thus, **5** was identified as the previously undescribed compound chrysoeriol 6-*C*-*β*-arabinofuranosyl-8-*C*-*β*-glucopyranoside (Fig. 4). A sodiated molecular ion $[M+Na]^+$ at *m/z* 617.14848 (calculated: 617.14832; Mass difference: 0.39 ppm) observed in the high resolution mass spectrum of **5** (Fig. S73) corresponding to $C_{27}H_{30}O_{15}Na$ confirmed this identity.

The 1D and 2D NMR spectra of **6** shared many similarities to that of **5**, showing chrysoeriol aglycone glycosylated with an arabinosyl unit at the 6-position and a glucopyranosyl substituent at the 8-position, respectively. The arabinosyl substituent of compound **6** was, however, determined to be in the pyranose form by the characteristic carbon signals at δ 73.9 (C-1″), δ 68.1 (C-2″), δ 73.6 (C-3″), δ 69.3 (C-4″) and δ 69.9 (C-5″) which are accord with an arabinopyranosyl unit (Fossen and Andersen, 2006). Thus, **6** was identified as the previously undescribed di-*C*-glycosylflavone chrysoeriol 6-*C*-*β*-arabinopyranosyl-8-*C*-*β*-glucopyranoside (Fig. 4). The sodiated molecular ion $[M+Na]^+$ at *m/z* 617.14867 (calculated: 617.14832; Mass difference: 0.71 ppm) observed in the high-resolution mass spectrum of **6** (Fig. S74) corresponding to $C_{27}H_{30}O_{15}Na$ confirmed this identity.

Two chrysoeriol di-C-glycosides found in quince seeds (*Cydonia oblonga* Miller) have previously been tentatively identified as chrysoeriol 6-*C*-pentosyl-8-*C*-glucoside and Chrysoeriol 6-*C*-pentosyl-8-*C*-glucoside by mass spectrometry (Ferreres et al., 2003; Silva et al., 2005), without identification of the pentose sugar unit. Interestingly, extracts of *Cydonia oblonga* seeds exhibited anticancer effect against human kidney and colon cancer cells (Carvalho et al., 2010). Salmenkallio et al. (1982) reported chrysoeriol 6-*C*-arabinosyl-8-*C*-glucoside from stems of *Trichophorum cespitosum*, without determining if the arabinosyl was present in the furanose or pyranose form. Chrysoeriol 6-*C*-arabinosyl-8-*C*-glucoside has also been indicated to occur in several *Arrhenaterum* spp. (Jay and Ismaili, 1989). No NMR data exist for these compounds in current literature, which would have allowed for the exact identification of the ring forms of their glycosyl substituents.

The 1D and 2D NMR spectra of **7** shared many similarities to that of **5**, showing chrysoeriol aglycone glycosylated with a pentose at the 6-position and a hexose at the 8-position, respectively. The 6-glycosyl substituent of **7** was identified as *β*-xylopyranose by comparing the five ^1H resonances in the region 4.55–3.05 in the 1D ^1H NMR spectrum of **7** and the corresponding five ^{13}C resonances belonging to this unit (Tables 4 and 5 and Supplementary Figs. S48–S51). The 8-glycosyl substituent of **6** was identified as *β*-galactopyranose by the signals corresponding to seven hydrogens in the region 5.00–3.47 in the 1D ^1H NMR spectrum of **7** and the corresponding six ^{13}C resonances belonging to this unit (Tables 4 and 5 and Supplementary Figs. S48–S51). The observed characteristic small axial-equatorial coupling constant for the coupling between H-3‴ and H-4‴ (2.8 Hz) verified the identification of the galactopyranose unit of **7**. Thus, **7** was identified as the previously undescribed compound chrysoeriol 6-*C*-*β*-xylopyranosyl-8-*C*-*β*-galactopyranoside) (Fig. 4). A sodiated molecular ion $[M+Na]^+$ at *m/z* of 617.14855 (calculated: 617.14832; Mass difference: 0.51 ppm) was observed in the high resolution mass spectrum of **7** corresponding to $C_{27}H_{30}O_{15}Na$. A further sodiated molecular ion $[M+2Na–H]^+$ at *m/z*

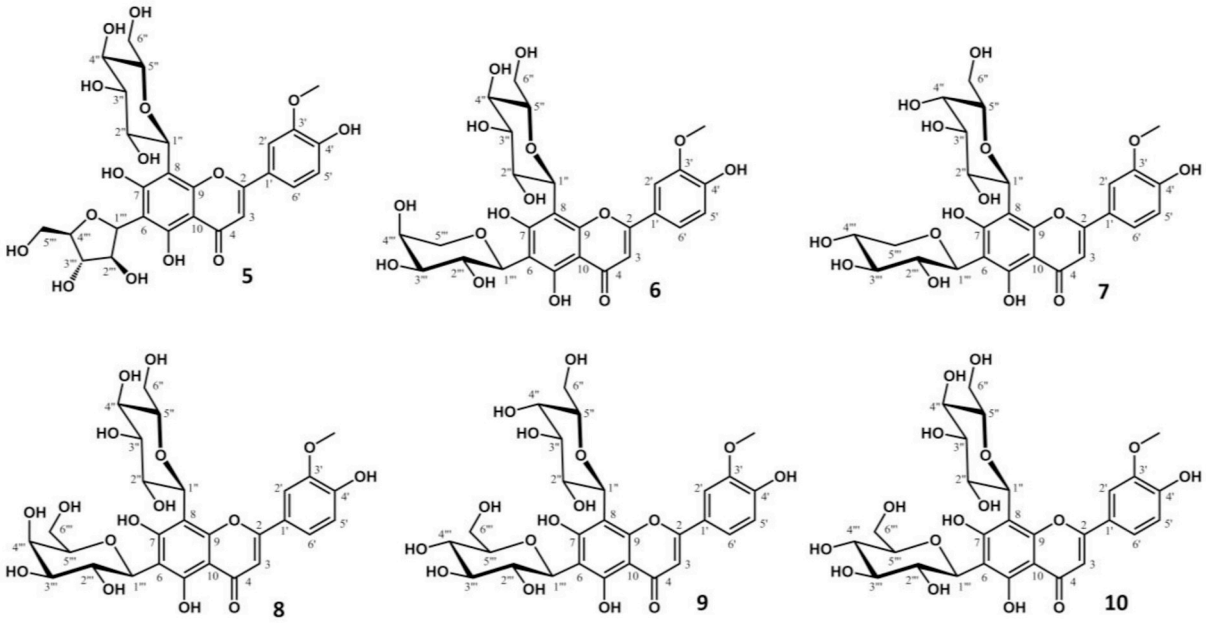

Fig. 4. Structures of the aromatic compounds chrysoeriol 6-*C*-*β*-arabinofuranosyl-8-*C*-*β*-glucopyranoside (**5**), chrysoeriol 6-*C*-*β*-arabinopyranosyl-8-*C*-*β*-glucopyranoside (**6**), chrysoeriol 6-*C*-*β*-xylopyranosyl-8-*C*-*β*-galactopyranoside (**7**), chrysoeriol 6-*C*-*β*-galactopyranosyl-8-*C*-*β*-glucopyranoside (**8**), chrysoeriol 6-*C*-*β*-glucopyranosyl-8-*C*-*β*-galactopyranoside (**9**) and chrysoeriol 6,8-di-*C*-*β*-*D*-glucopyranoside (**10**) isolated for the first time from flowering tops of *N. ossifragum*.

Table 4
^{1}H NMR chemical shift values (ppm) and coupling constants (Hz) of chrysoeriol 6-*C*-*β*-arabinofuranosyl-8-*C*-*β*-glucopyranoside (**5**), chrysoeriol 6-*C*-*β*-arabinopyranosyl-8-*C*-*β*-glucopyranoside (**6**), chrysoeriol 6-*C*-*β*-xylopyranosyl-8-*C*-*β*-galactopyranoside (**7**), chrysoeriol 6-*C*-*β*-galactopyranosyl-8-*C*-*β*-glucopyranoside (**8**), chrysoeriol 6-*C*-*β*-glucopyranosyl-8-*C*-*β*-galactopyranoside (**9**) and chrysoeriol 6,8-di-*C*-*β*-*D*-glucopyranoside (**10**) in DMSO-D_6 at 298K. Top: Signals of major rotamer. Bottom: Signals of minor rotamer. s = singlet; d = doublet; dd = double doublet; ddd = double double doublet; t = triplet; br = broad; m = multiplet.

	5	6	7	8	9	10
3	6.94 *s*	6.94 *s*	6.86 *s*	6.94 *s* (6.91 *s*)	6.86 *s* (7.00 *s*)	6.95 (6.87)
2'	7.55 *d* 2.2	7.54 *d* 2.2	7.65 *d* 2.1	7.54 *d* 2.3 (7.59 *d* 2.2)	7.65 *d* 2.2 (7.56)	7.55 (7.64)
5'	6.88 *d* 8.3	6.89 *d* 8.4	6.92 *d* 8.4	6.89 *d* 8.4 (6.95)	6.92 *d* 8.4 (6.88)	6.88 (6.95)
6'	7.73 dd 8.3, 2.2	7.70 dd 8.4, 2.2	7.58 dd 8.4, 2.1	7.70 dd 8.4, 2.3 (7.56 dd 8.4, 2.2)	7.58 dd 8.4, 2.2 (8.27)	7.71 (7.57)
5-OH	13.81 *s*	13.71	13.74	13.71 *s*	13.75 *s* (13.86 *s*)	13.75 (13.73)
7-OH	10.52 *s*	9.18	9.23	9.18 *s*	9.24 *s* (br) (9.03 *s* (br))	9.36 (9.36)
4'-OH	10.00 *s*	9.99 *s*	9.96	10.00 *s*	9.96 *s* (9.83 *s*)	
3'-OCH_3	3.88 *s*	3.88 *s*	3.90 *s*	3.88 *s* (3.90 *s*)	3.90 *s* (3.88 *s*)	3.88 *s* (3.90 *s*)
	6-*C*-*β*-Arabinofuranosyl	**6-*C*-*β*-Arabinopyranosyl**	**6-*C*-*β*-Xylopyranosyl**	**6-*C*-*β*-Galactopyranosyl**	**6-*C*-*β*-Glucopyranosyl**	**6-*C*-*β*-Glucopyranosyl**
1''	5.44 *d* 3.2	4.71 *d* 9.2	4.55 *d* 9.8	4.77*d* 9.7 (4.70 d 9.7)	4.62 *d* 10.0 (4.80)	4.80 *d* 9.9 (4.66 *d*)
2''	4.09 dd 3.2, 0.8	3.80 *m*	4.09 *m*	3.80 dd 9.7, 9.5	4.12 (3.48 (br))	3.48 *m* (3.98)
3''	3.93 dd 3.0, 0.8	3.46 *m*	3.13 *t* 8.7	3.45 *m*	3.19 *t* 8.6 (3.30)	3.30 *t* 8.8 (3.22)
4''	3.89 *m*	3.81 *m*	3.38 *m*	3.79	3.08 *t* 9.0	3.37 *t* 9.4
5A''	3.67 dd 11.3, 6.6,	3.83 dd 11.9, 2.7	3.74 *m*	3.56	3.15 *m* (3.32)	3.32 *m*
5B''	3.64 dd 4.8, 11.3	3.64 *d* 11.9	3.05 *t* 10.8			
6A''				3.53 *m*	3.70 dd 12.0, 2.0 (3.63)	3.63 *m*
6B''					3.37 *m*	
	8-*C*-*β*-Glucopyranoside	**8-*C*-*β*-Glucopyranoside**	**8-*C*-*β*-Galactopyranoside**	**8-*C*-*β*-Glucopyranoside**	**8-*C*-*β*-Galactopyranoside**	**8-*C*-*β*-Glucopyranoside**
1'''	4.70 *d* 9.9	4.74 *d* 9.8	5.00 *d* 9.6	4.74 *d* 10.00 (4.91 d 10.0)	5.00 *d* 9.6 (4.69 *d* 9.9)	4.75 *d* 9.9 (5.04 *d*)
2'''	3.88 *m*	3.93 dd 9.8, 8.7	3.80 *t* 9.3	3.94 dd 10.0, 9.0 (3.89)	3.83 *m* (4.24 *t* 9.4)	3.92 dd 9.8, 8.7, (3.56)
3'''	3.24 *t* 8.8	3.27 *t* 8.7	3.47 dd 9.3, 2.8	3.27 *t* 8.8	3.47 dd 9.1, 3.9 (3.41 dd 8.9, 3.2)	3.26 *t* 8.7 (3.31)
4'''	3.35 dd 9.6, 8.8	3.36 dd 9.6, 8.7	3.83 *d* 2.8	3.34 dd 9.6, 8.8	3.83 *br d* 2.9 (3.85)	3.34 *t* 9.1 (3.34)
5'''	3.23 ddd 9.6, 6.1, 2.1	3.23 ddd 9.6, 6.0, 2.0	3.71 *t* 6.2	3.23 ddd 9.6, 6.3, 2.0	3.71 *m*	3.22 ddd 9.5, 6.2, 1.9 (3.18)
6A'''	3.76 dd 12.1, 2.1	3.73 dd 12.1, 2.0	3.55 *d* 6.2	3.75 dd 12.4, 2.0 (3.71)	3.56 *m* (3.56)	3.74 dd 12.0, 1.9 (3.69)
6B'''	3.48 dd 12.1, 6.1	3.47 dd 12.1, 6.0		3.46 dd 12.1, 6.3 (3.46)		3.47 dd 12.0, 6.2 (3.46)

*proton signals overlapping in the 1D ^{1}H NMR spectra are reported without designated multiplicity.

Table 5
^{13}C NMR chemical shift values (ppm) and coupling constants (Hz) of chrysoeriol 6-*C*-*β*-arabinofuranosyl-8-*C*-*β*-glucopyranoside (**5**), chrysoeriol 6-*C*-*β*-arabinopyranosyl-8-*C*-*β*-glucopyranoside (**6**), chrysoeriol 6-*C*-*β*-xylopyranosyl-8-*C*-*β*-galactopyranoside (**7**), chrysoeriol 6-*C*-*β*-galactopyranosyl-8-*C*-*β*-glucopyranoside (**8**), chrysoeriol 6-*C*-*β*-glucopyranosyl-8-*C*-*β*-galactopyranoside (**9**) and chrysoeriol 6,8-di-*C*-*β*-*D*-glucopyranoside (**10**) in DMSO-D_6 at 298K. Top: Signals of major rotamer. Bottom: Signals of minor rotamer. nd = not detected.

	5	6	7	8	9	10
Chrysoeriol						
2	164.0	163.9	163.2	164.1 (163.5)	163.2 (164.1)	164.1 (163.5)
3	102.8	103.0	102.6	103.0 (102.8)	102.6 (103.4)	103.1 (102.8)
4	182.2	182.1	181.9	182.2 (182.2)	182.2 (182.2)	182.5 (182.4)
5	157.1	158.0	159.8	158.1	nd (158.5)	158.6 (159.9)
6	103.3	107.9	109.1	108.2	109.2 (107.1)	107.6 (109.0)
7	162.7	160.7	161.4	160.8	161.5 (160.7)	160.9 (161.5)
8	104.5	104.7	103.8	105.0	103.4 (105.2)	105.3
9	154.9	155.1	153.1	155.1	153.2 (155.2)	155.1
10	103.1	103.5	102.9	103.6 (102.9)	103.0 (103.8)	103.7 (103.3)
1’	121.9	121.6	121.5	121.7 (121.6)	121.4 (120.9)	121.8 (121.7)
2’	110.6	110.5	110.0	110.7 (109.9)	110.1 (109.9)	110.7 (110.2)
3’	148.0	147.8	147.8	148.0 (147.9)	147.7 (147.7)	148.1 (147.8)
4’	150.8	150.6	150.3	150.8 (150.5)	150.3 (150.6)	150.9 (150.4)
5’	115.5	115.1	115.4	115.4 (115.8)	115.6 (115.7)	115.5 (115.7)
6’	121.2	121.0	120.5	121.1 (120.3)	120.3 (123.0)	121.3 (120.5)
3′-OCH_3	56.2	56	55.5	56.1 (55.6)	55.6 (55.9)	56.2 (55.7)
	6-*C*-*β*-Arabinofuranosyl	**6-*C*-*β*-Arabinopyranosyl**	**6-*C*-*β*-Xylopyranosyl**	**6-*C*-*β*-Galactopyranosyl**	**6-*C*-*β*-Glucopyranosyl**	**6-*C*-*β*-Glucopyranosyl**
1’’	79.9	73.9	73.4	73.5 (73.6)	72.7 (73.9)	74.0 (73.1)
2’’	77.3	68.1	77.2	69.6 (68.5)	69.7 (71.8)	71.9
3’’	77.4	73.6	79.1	74.4 (74.7)	79.1 (77.7)	77.8 (78.9)
4’’	87.0	69.3	69.7	68.3	70.7	69.0
5’’	61.1	69.9	70.0	79.0	81.7 80.7)	80.9
6’’				60.7	61.5 (59.7)	59.7
	8-*C*-*β*-Glucopyranoside	**8-*C*-*β*-Glucopyranoside**	**8-*C*-*β*-Galactopyranoside**	**8-*C*-*β*-Glucopyranoside**	**8-*C*-*β*-Galactopyranoside**	**8-*C*-*β*-Glucopyranoside**
1’’’	73.0	72.9	74.8	73.0 (74.5)	74.9 (73.7)	73.2 (75.1)
2’’’	70.7	70.6	69.8	70.7 (70.7)	68.2 (68.8)	70.8 (72.0)
3’’’	78.7	78.7	74.3	78.8 (79.0)	74.4 (75.5)	78.8 (78.3)
4’’’	70.5	70.4	68.1	70.6 (70.5)	69.7 (69.1)	70.6 (69.2)
5’’’	81.9	81.7	79.2	81.9 (82.0)	79.4	82.0 (81.8)
6’’’	61.4	61.1	60.5	61.3 (61.6)	60.7 (60.8)	61.3 (61.3)

639.13064 (calculated: 639.13027; Mass difference: 0.71 ppm) observed in the high resolution mass spectrum of **7** corresponding to $C_{27}H_{29}O_{15}Na_2$ confirmed this identification.

The 1D and 2D NMR spectra of **9** shared many similarities to that of **7**, showing chrysoeriol aglycone glycosylated at positions 6 and 8 of the aglycone, with galactopyranose as the 8-glycosyl substituent (Fig. 4 and Tables 4 and 5). The 6-*C*-glycosyl substituent of **9** was, however, identified as glucopyranosyl (Fig. 4 structure and Tables 4 and 5). Thus, **9** was identified as the previously undescribed flavonoid chrysoeriol 6-*C*-*β*-glucopyranosyl-8-*C*-*β*-galactopyranoside) (Fig. 4). The sodiated molecular ion $[M+Na]^+$ at *m/z* 647.15899 (calculated: 647.15889; Mass difference: 0.29 ppm) observed in the high resolution mass spectrum corresponding to $C_{28}H_{32}O_{16}Na$, and $[M+2Na–H]^+$ at *m/z* 669.14084 (calculated: 669.14084; Mass difference: 0.34 ppm) observed in the high resolution mass spectrum of **9** (Fig. S77) corresponding to $C_{28}H_{31}O_{16}Na_2$ confirmed this identification.

The 1D and 2D NMR spectra of **8** shared many similarities to that of **9**, showing chrysoeriol aglycone *C*-glycosylated with glucose and galactose at positions 6 and 8 of the aglycone, although the positions of the *C*-glycosyl substituents were interchanged as compared to those of **9**. Thus, **8** was identified as the previously undescribed flavonoid chrysoeriol 6-*C*-*β*-galactopyranosyl-8-*C*-*β*-glucopyranoside (Fig. 4). The sodiated molecular ions $[M+Na]^+$ at *m/z* 647.15868 (calculated: 647.15889; Mass difference: −0.19 ppm) observed in the high resolution mass spectrum (Fig. S76) of **8** corresponding to $C_{28}H_{32}O_{16}Na$, and $[M+2Na–H]^+$ at *m/z* 669.14138 (calculated: 669.14084; Mass difference: 0.94 ppm) corresponding to $C_{28}H_{31}O_{16}Na_2$ confirmed **8** to be the previously undescribed compound chrysoeriol 6-*C*-*β*-galactopyranosyl-8-*C*-*β*-glucopyranoside.

Circular Dichroism (CD) spectra of all isolated di-*C*-glycosylflavones were recorded. All these compounds are based on the same chrysoeriol aglycone. According to Gaffield et al. (1978) the CD bands of di-*C*-glycosylflavones are often relatively weak as a result of overlapping of oppositely signed adjacent CD bands (Wellman et al., 1965). The similarity of the recorded CD spectra of compounds **6–10** indicate that the configurations of C-1 of the glycosyl substituents are similar for these compounds (Gaffield et al., 1978). The fact that the CD spectrum of compound **5**, which exhibited a strong negative band at 275 nm, differed from the CD-spectra recorded of compounds **6–10** may not be unexpected since compound **5** is the only di-*C*-glycosylflavone among the isolated compounds which is substituted by an arabinofuranosyl moiety.

Compounds **8–10** exhibit most of their ^{1}H and ^{13}C-NMR signals (Tables 4 and 5) in double sets. These signals reveal two conformational isomers created by rotational hindrance at the *C* (sp^3)–*C* (sp^2) glucosyl–flavone linkage in each of these 6,8-di-C-substituted flavones (Rayyan et al., 2005). The equilibrium between the rotamers was supported by observations of strong exchange peaks between equivalent protons of each of the rotameric pairs in their ROESY spectra (Supplementary Fig. S57, S63 and S69).

Isomerisation of di-*C*-glycosyl flavones by Wessely Moser rearrangement was demonstrated to occur by the fact that during the final isolation of pure compounds by preparative HPLC, compound **5** was isolated at two different retention times from the same mixture. This

Table 6
Cytotoxicity of compounds **1–10** against three mammalian cell lines. The compounds were diluted in DMSO or water and a dilution series made on each cell line. The cells were tested for metabolic activity after 72 h of incubation. The EC_{50} values were determined by non-linear regression from 3 to 5 independent experiments (NRK and MOLM13) as described in the methods section. The data from H9c2 is from one experiment. "– " denotes that no data is available due to low toxicity.

	NRK		Molm13		H9c2	
	EC_{50} (mM)	R^2	EC_{50} (mM)	R^2	EC_{50} (mM)	R^2
1	0.5–1	–	0.4	0.66	> 0.3	–
2	0.12	0.86	0.22	0.69	0.2–0.6	–
3	0.05	0.77	0.08	0.74	0.02	0.92
4	0.007	0.94	0.002	0.85	0.006	0.96
5	> 1	–	0.5–1.0	–	–	–
6	> 1	–	0.5–1.0	–	–	–
7	> 1	–	> 1	–	–	–
8	> 1	–	> 1	–	–	–
9	> 1	–	> 1	–	–	–
10	> 1	–	0.5–1	–	–	–

may not be surprising since we have previously observed similar isomerisation of *C*-glycosyl-3-deoxyanthocyanins occurring under similar mild experimental conditions (Bjorøy et al. 2009a, 2009b).

To investigate if any of the compounds could be responsible for the death of sheep and cattle, their cytotoxic potential was investigated on three cell lines. The rat kidney epithelial cell line NRK, the rat cardiomyoblast H9c2, and the human AML cell line Molm13. The flavonoids (compounds **5–10**) exhibited no, or very low toxicity towards the cell lines, with either activity above 0.5 mM, or no detectable cytotoxic activity at 1 mM (Table 6). The saponins (compounds **1–4**) were more potent. Interestingly, the cytotoxic potential increased proportionally with the increasing number of glycosyl substituents, where compound **4** (sarsasapogenin-3-*O*-(2′-*O*-*β*-glucopyranosyl-3′-*O*-*α*-arabinopyranosyl-*β*-galactopyranoside)) showed an EC_{50} (concentration leading to 50% cell death) between 2 and 8 μM after 72 h of incubation (Table 6 and Fig. 5). Incubation time for 24 h gave higher EC_{50} values (Table 6 and Fig. 5), but for compound **4**, the EC_{50} values for the different cell lines were still between 3 and 10 μM.

The results presented in Table 6 and Fig. 5 indicate that the saponins, and particularly the main saponin, compound **4**, are responsible for some of the toxic effects observed in livestock after ingestion of flowering tops of *N. ossifragum.* All cell lines were severely affected by the main saponin compound **4**, indicating that the presence of this substance in the vascular system might affect the function of the heart, leukocytes, and kidneys. Furthermore, our data suggests that compounds **3** and **4** induce both a sub-acute and protracted toxicity, since we found significant cell death at 24 h, which increased after 72 h (Fig. 5). It has previously been shown that orally administered saponins induced damage in the intestinal mucosa, as well as causing liver and kidney necrosis (Aguilar-Santamaría et al. (2013); Diwan et al. (2000)). Moreover, case reports of cattle with suspected *N. ossifragum* poisoning showed hepatic fibrosis and reduced renal function (Flåøyen et al., 1995a Flåøyen et al., 1995b; Angell and Ross (2011)). Interestingly, Angell and Ross (2011) observed that the condition of one of the cattle exacerbated even after treatment was initiated (Angell and Ross, 2011), indicating irreparable damage, or a protracted toxic effect. The kidney and liver might be particularly vulnerable to compounds like compound **3** and **4** due to their high perfusion rate, and their ability to actively take up (hepatocytes) or concentrate (kidney tubules) xenobiotics.

3. Concluding remarks

For the first time, saponins from *N. ossifragum* have been characterized at atomic resolution. The cytotoxicity of the saponins

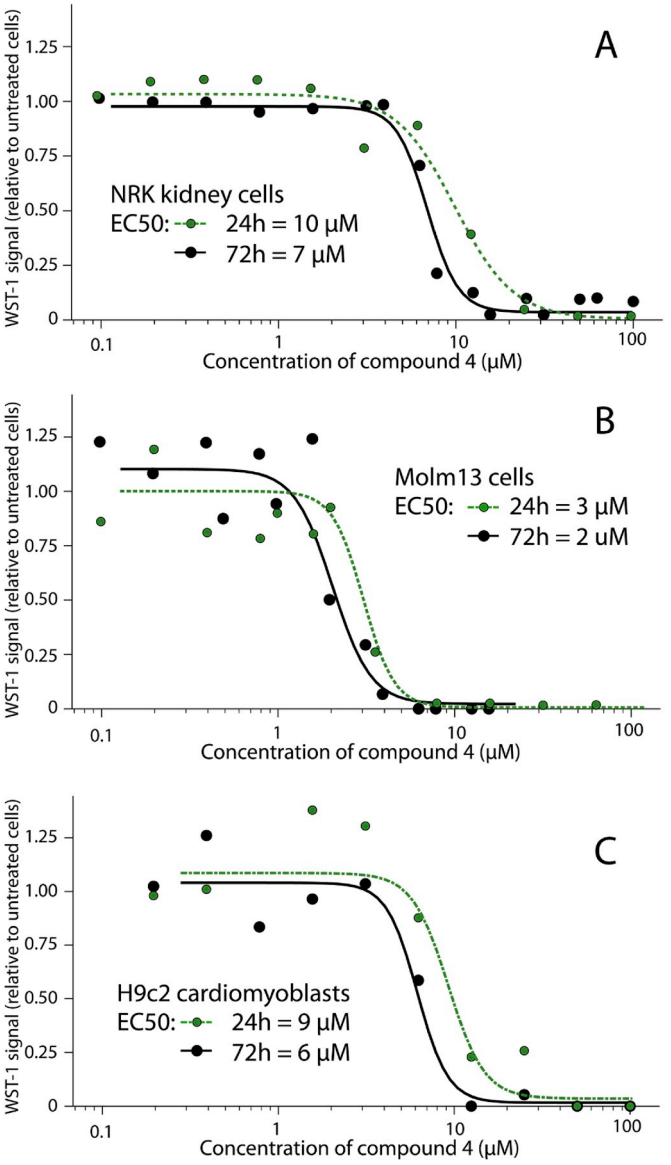

Fig. 5. EC_{50} values of the main saponin (**4**) isolated from flowering tops of *N. ossifragum* towards normal rat kidney (NRK) cells, MOLM13 cells and H9c2 cardiomyoblasts.

increased proportionally with the increasing number of glycosyl substituents. The fact that the main saponin, sarsasapogenin-3-*O*-(2′-*O*-*β*-glucopyranosyl-3′-*O*-*α*-arabinopyranosyl-*β*-galactopyranoside) (**4**), which comprises several percent of the dry weight of flowering tops of *N. ossifragum*, proved to be the main toxic principle towards all tested cell lines may indicate that this compound is responsible for the observed kidney and liver damage seen in cattle after ingestion of *N. ossifragum*. The fact that the structures of the saponins of *N. ossifragum* have now been determined, in addition to the presentation of a protocol for large-scale isolation of these compounds paves the way for further extensive structure-activity studies of these compounds. Even although the flowering tops of *N. ossifragum* have been indicated to contain the causative agents of the phototoxic disease alveld, no aromatic compounds have previously been identified therefrom. Here, we report on the detailed characterization of five di-*C*-glycosylflavones, which have been completely characterized for the first time, in addition to a structurally related known compound.

4. Experimental

4.1. Plant material

Fresh plant material of *Narthecium ossifragum* (L.) Huds. (Nartheciaceae) was collected in the summer season (collection date 07/2016) in a bog area located at south western part of Ulriken, Bergen, Norway at 350m above sea level (coordinates 60.36884N 005.38237E). Voucher specimen of *N. ossifragum* has been deposited at the ARBOHA, University of Bergen (accession number BG/S-162115). Prior to extraction, the plant material was stored at −80 °C. The water content of the plant material was determined to be 81.3% of the weight.

4.2. Extraction of compounds and partitions with organic solvents

Flowering tops (1.7 kg) of *N. ossifragum* were extracted with 15 L methanol for 72 h at room temperature. The extraction yield was 7.6% of the wet weight. When taking into account that the water content was 81.3%, the dry weight extraction yield was 40.5%. The methanolic extract was filtered through glass wool and concentrated by rotary evaporator under reduced pressure. The resulting concentrated aqueous extract was partitioned (three times) with petroleum ether (3 L), followed by partition (three times) with ethyl acetate (3 L). The residual aqueous phase was concentrated by rotavapor to a volume of 500 mL. The petroleum ether and the ethyl acetate phases provided a white precipitate, which was collected and dried before further purification and separation as described below.

4.3. Amberlite XAD-7 column chromatography

The concentrated residual aqueous partition (500 mL) was applied to an Amberlite XAD-7 column (column dimensions 50 × 1000 mm, containing 500g XAD-7 stationary phase). The mobile phase gradient consisted of 5 L distilled water (fractions 1–5), followed by 1L water-methanol 90:10; v/v (fraction 6), 1 L water-methanol 75:25; v/v (fraction 7), 3 L water-methanol 50:50; v/v (fraction 8–10) and finally 4 L methanol 100% (fractions 11–14). The flow rate was 5 mL/min. This gave a total of 14 fractions with volumes of 1 L, which were analysed individually by analytical HPLC.

4.4. Sephadex LH-20 column chromatography

Fractions 8–10 from the Amberlite XAD-7 column chromatography were combined, concentrated to a volume of 20 mL and further separated on a Sephadex LH-20 column (column dimensions 50 × 1000 mm, containing 500 g Sephadex LH-20 stationary phase) using a gradient of water and methanol containing 0.2% of TFA. The gradient consisted of 650 mL water-methanol-TFA 80:20:0.2; v/v/v (fractions 1–13), followed by 900 mL water-methanol-TFA 50:50:0.2 v/v/v (fractions 14–32) and finally 800 mL water-methanol-TFA 30:70:0.2 v/v/v (fractions 33–49). The flow rate was 5 mL/min. A total of 49 fractions, each with a volume of 50 mL were collected.

4.5. Preparative HPLC

Compounds of the combined fractions 4–6 from the Sephadex LH-20 column chromatography were isolated by preparative HPLC (Gilson 321 preparative HPLC equipped with a Dionex Ultimate 3000 variable wavelength detector). The HPLC instrument was equipped with a C_{18} Ascentis column (250 × 20 mm; 5 µm, spherical particles). Chromatograms were recorded at 360 nm. Two solvents were used for elution; mobile phase A (water-TFA 99.9:0.1 v/v) and mobile phase B (methanol-TFA 99.9:0.1 v/v). The flow rate was 12 mL/min. Prior the analysis the combined fractions were evaporated to dryness and dissolved in a mixture of 1:1; v/v of the two mobile phases. Portions of 200 µL were manually injected into the HPLC column. Fractions were collected manually based on peaks appearing in the on-line chromatogram recorded at 360 nm. The collected fractions were transferred to HPLC vials for purity control using analytical HPLC. Following this strategy 16.4 mg of compound **5**, 6.2 mg of compound **6**, 1.8 mg of compound **7**, 3.4 mg of compound **8**, 8.5 mg of compound **9** and 2.2 mg of compound **10** were obtained.

4.6. Analytical HPLC

The HPLC instrument (Dionex P680) was equipped with a multidiode array detector, an autoinjector and a 250 × 4.6 mm, 5 µm Thermo Scientific Hypersil GOLD column. Two solvents were used for elution; A (water-TFA 99.5:0.5; v/v) and B (acetonitrile-TFA 99.5:0.5; v/v). The flow rate was 1 mL/min. Aliquots of 20 µl were injected.

4.7. Isolation of pure saponins from crystallized mixture of saponins

7.1546 g of crystals from the extract of flowering tops of *N. ossifragum* were precipitated and collected from the concentrated petroleum ether and ethyl acetate partitions of the crude extract. The 1D and 2D NMR spectra of 20 mg of these crystals dissolved in DMSO-D_6 indicated that they consisted of a mixture of saponins. Subsequently, 1g of these crystals was dissolved in 5 mL of DMSO and further purified by Sephadex LH-20 chromatography.

4.8. Purification of saponins by Sephadex LH-20 column chromatography

1 g of crystals dissolved in 5 mL DMSO was purified on a Sephadex LH-20 column (500 × 50 mm containing 200 g column material) using a gradient of 600 mL water-methanol-TFA 50:50:0.2 v/v/v, followed by 4450 mL of methanol-TFA 100:0.2 and finally 1750 mL of acetone 100%. The flow rate was 5 mL/min 138 fractions, each with volumes of 25 mL, were collected, evaporated to dryness under nitrogen and analysed by TLC.

4.9. Silica gel column chromatography

Fractions 35–55 from the Sephadex LH-20 column chromatography were combined, concentrated to a volume of 5 mL and further separated on a Silica gel column (200 × 50 mm containing 300 g column material) using a gradient of ethyl acetate-methanol-water as mobile phase. The gradient consisted of 3000 mL of ethyl acetate-methanol-water 80:20:4 v/v/v, followed by 3000 mL ethyl acetate-methanol-water 50:50:4; v/v/v and finally by 575 mL of ethyl acetate-methanol-water 20:80:4; v/v/v. The flow rate was 8 mL/min. The silica chromatographic separation resulted in collection of 275 fractions, each with a volume of 25 mL. The resulting fractions were concentrated to dryness under nitrogen and analysed by TLC. Following this strategy 4.6 mg of sarsasapogenin (**1**), 13.1 mg of sarsapogenin-3-*O*-*β*-galactopyranoside (**2**), 56.1 mg of sarsasapogenin-3-O-(2′-*O*-*β*-glucopyranosyl)-*β*-galactopyranoside (**3**), and 260.7 mg of sarsapogenin-3-*O*-*β*-(2′-*O*-*β*-glucopyranosyl-3′-*O*-*α*-arabinopyranosyl-*β*-galactopyranoside) (**4**) were obtained.

4.10. Analytical TLC

Purified mixtures of saponins and isolated pure saponins were analysed by a TLC method modified from the procedures described by Kobayashi et al., 1993 and Miles et al., 1991. The chromatographic separation was performed on silica TLC plates. The mobile phase consisted of ethyl acetate-methanol-water 80:20:4; v/v/v. Detection of colourless compounds after TLC separation was achieved using Ehrlich's solution (4-(dimethylamino)benzaldehyde in hydrochloric acid solution provided by Sigma Aldrich) and 5% sulfuric acid on methanol as spray reagent.

4.11. Spectroscopy

High resolution mass spectra were recorded using a JEOL AccuTOF JMS T100LC instrument fitted with an electrospray ion source. The spectrum was recorded over the mass range 50–1000 *m/z*.

UV–Vis absorption spectra were recorded on-line during HPLC analysis over the wavelength range 240–600 nm in steps of 2 nm.

Specific rotations of compounds **1–4** were determine on a Rudolph Research Analytical Autopol IV instrument. Samples dissolved in DMSO were transferred to a 600 µl cell. Measurements were performed at 589 nm. The specific rotations were determined to be −2.86° for compound **4**, -22.33° for compound **3**, -10.83° for compound **2** and -2.00° for compound **1**.

Circular Dichroism (CD) spectra were recorded at 20 °C in a Jasco J-810 spectropolarimeter equipped with a Peltier temperature control unit. 5 mM of compounds **5**, **7** and **9**, 1 mM of compounds **6** and **8** and 0.5 mM of compound 10 solubilised in 100% DMSO were used to obtain the spectra. The spectra obtained were the average of 6 scans. Buffer scans (100% DMSO) were subtracted from the spectra. The spectra were scanned from 185 nm to 450 nm, but only the relevant region of the scans (250–400 nm) is shown. A 1-mm pathlength cell was used.

NMR samples were prepared by dissolving the isolated compounds in deuterated dimethylsulfoxide (DMSO-D_6; 99.96 atom % D, Sigma-Aldrich). The 1D ^{1}H and the 2D ^{1}H–^{13}C HMBC, the 2D ^{1}H–^{13}C HSQC, the 2D ^{1}H–^{13}C HSQC-TOCSY, the 2D ^{1}H–^{13}C H2BC, the 2D ^{1}H–^{1}H COSY and 2D ^{1}H–^{1}H ROESY NMR experiments were obtained at 850 MHz at 298K on a Bruker 850 MHz instrument equipped with a ^{1}H,^{13}C,^{15}N triple resonance cryogenic probe.

4.12. Brine shrimp lethality assay

The stock solution was prepared by dissolving 124 mg of the crystallized mixtures of saponins in 1 mL DMSO. 20 µL of this stock solution was transferred to a beaker containing 10 mL of seawater (distilled water containing 35.5 g/l dissolved sea salt) to make the stock solution. A volume of 0, 2, 5, 7, 9, 12.5 µL of the stock solution of saponin were used in each well containing 10–20 *Artemia salina* nauplii, having a total volume of 200 µL seawater. Individual concentrations in each well were 2.5, 5, 8.8, 11.3 and 15.6 µg/mL, respectively. Three parallels of each concentration and controls were performed. After 24 h the number of surviving *A. salina* nauplii in each well were counted using a computer-connected Veho 400x USB microscope with 20 times magnification.

4.13. Cytotoxicity towards mammalian cell lines

Stock solutions were prepared by dissolving pure compounds to a final concentration of 100 mM in DMSO. The normal rat kidney epithelial cells (NRK, ATCC no.: CRL-6509) and rat cardiomyoblasts (H9c2, ATCC no.: CRL-1446) were cultured in DMEM supplemented with 10% fetal bovine serum (FBS, Invitrogen, Carlsbad, CA). When the cells reached 80% confluence, they were detached by mild trypsin treatment (0.33 mg/mL trypsin for 5 min at 37 °C), centrifuged (160 × *g*, 4 min) and reseeded in fresh medium to 25% confluence. The AML cell line MOLM13 (Matsuo et al., 1997; Quentmeier et al., 2003) were cultured in RPMI 1640 medium enriched with 10% FBS. The cells were kept in suspension cultures at a density of between 150,000 and 600,000 cells/mL. All media were supplemented with 1 IU/mL penicillin and 1 mg/mL streptomycin (both from Cambrex, Belgium), and incubated in a humidified atmosphere (37 °C, 5% CO_2).

For cytotoxicity experiments with compounds **1–10**, the NRK and H9c2 cells were seeded in 96 well tissue culture plates (5000 cells/well, 0.1 mL) and left overnight to attach before adding compounds. The MOLM13 cells were seeded in 96 well tissue culture plates at 15,000 cells/well in 0.1 mL on the day of the experiment. Compounds dissolved in DMSO were added to the cells, and the plates were kept overnight before addition of the tetrazolium salt WST-1 according to the manufacturer instructions. The plates were further incubated for 2 h before the signal was recorded at 450 nm with reference at 620 nm. For blank subtraction, medium added only WST-1 and compound was used. In some of the experiments involving coloured compounds, the fluorescent dye resazurin, which is converted to the reporter product by the same enzyme as WST-1, was used as an alternative. The protocol is identical, except that viability was assessed by measuring fluorescence at 480/520 nm. After recording of WST-1 or resazurin conversion, the cells were next fixed 2% buffered formaldehyde (pH 7.4) with 0.01 mg/mL of the DNA-specific fluorescent dye, Hoechst 33342. The presence of dead (apoptotic or necrotic) cells was verified by differential interference contrast and fluorescence microscopy as previously described (Oftedal et al., 2010; Myhren et al., 2014). EC_{50} values were determined by a four-parameter regression analysis as described previously (Viktorsson et al. (2017)), using IBM SPSS® statistic software (ver. 25). For comparison the corresponding EC_{50} values of the standard compound quercetin 3-(6″-rhamnosylglucoside) (rutin) was 40 ± 12 µM for MOLM13 cells and 245 ± 19 µM for NRK cells.

Acknowledgements

The authors acknowledge Dr. Bjarte Holmelid for recording the high-resolution mass spectra, Professor George W. Francis for proofreading the manuscript and Centre for Pharmacy at the University of Bergen, the Western Norway Health authorities (912052), and the Norwegian Cancer Society (112502) for financial support. This work was partly supported by the Research Council of Norway through the (226244/F50).

Appendix A. Supplementary data

Supplementary data to this article can be found online at https://doi.org/10.1016/j.phytochem.2019.04.014.

References

Abdelkader, S.V., Ceh, L., Dishington, I.W., Hauge, J.G., 1984. Alveld-producing saponins. II: toxicological studies. Acta Vet. Scand. 25, 76–85.

Aguilar-Santamaría, L., Herrera-Arellano, A., Zamilpa, A., Alonso-Cortés, D., Jiménez-Ferrer, E., Tortoriello, J., Zúñiga-González, G., 2013. Toxicity, genotoxicity, and cytotoxicity of three extracts of *Solanum chrysotrichum*. J. Ethnopharmacol. 150, 275–279.

Angell, J., Ross, T., 2011. Suspected bog asphodel (*Narthecium ossifragum*) toxicity in cattle in North Wales. Vet. Rec. 169, 101. https://doi.org/10.1136/vr.d3879.

Bernhoft, A. (Ed.), 2010. Bioactive Compounds in Plants - Benefits and Risks for Man and Animals. The Norwegian Academy of Science and Letters, Oslo, Norway (Novus forlag, Oslo).

Bjorøy, Ø., Rayyan, S., Fossen, T., Kalberg, K., Andersen, Ø.M., 2009a. Anthocyanin *C*-glycosides from flavone *C*-glycosides. Phytochemistry 70, 278–287.

Bjorøy, Ø., Rayyan, S., Fossen, T., Andersen, Ø.M., 2009b. Detailed properties of anthocyanins – rearrangement of *C*-glycosyl-3-deoxyanthocyanidins in acidic aqueous solutions. J. Agric. Food Chem. 57, 6668–6677.

Bouillant, M.-L., Ferreres de Arce, F., Favre-Bonvin, J., Chopin, J., Zoll, A., Mathieu, G., 1979. Nouvelles *C*-glycosylflavones extraites de *Spergularia rubra*. Phytochemistry 18, 1043–1047.

Carvalho, M., Silva, B.M., Silva, R., Valentao, P., Andrade, P.B., Bastos, M.L., 2010. First report on *Cydonia oblonga* Miller anticancer potential: differential antiproliferative effect against human kidney and colon cancer cells. J. Agric. Food Chem. 58, 3366–3370.

Ceh, L., Hauge, J.G., 1981. Alveld-producing saponins. I. Chemical studies. Acta Vet. Scand. 22, 391–402.

di Menna, M.E., Flåøyen, A., Ulvund, M.J., 1992. Fungi on *Narthecium ossifragum* leaves and their potential involvement in alveld disease of Norwegian lambs. Vet. Res. Commun. 16, 117–124.

Diwan, F.H., Abdel-Hassan, I.A., Mohammed, S.T., 2000. Effect of saponin on mortality and histopathological changes in mice. East. Mediterr. Health J. 6, 345–351.

Feilberg, J., 1999. Blomster I Norge. Aschehoug, Oslo.

Ferreres, F., Silva, B.M., Andrade, P.B., Seabra, R.M., Ferreira, M.A., 2003. Approach to the study of *C*-glycosyl flavones by ion trap HPLC-PAD-ESI/MS/MS: application so seeds of quince (*Cydonia oblonga*). Phytochem. Anal. 14, 352–359.

Flåøyen, A., Hjorth Tønnesen, H., Grønstøl, H., Karlsen, J., 1991. Failure to induce toxicity in lambs by administering saponins from *Narthecium ossifragum*. Vet. Res. Commun. 15, 483–487.

Flåøyen, A., Bratberg, B., Frøslie, A., Grønstøl, H., 1995a. Nephrotoxicity and hepatotoxicity in calves apparently caused by experimental feeding with *Narthecium ossifragum*. Vet. Res. Commun. 19, 63–73.
Flåøyen, A., Binde, M., Bratberg, B., Djønne, B., Fjølstad, M., Grønstøl, H., Hassan, H., Mantle, P.G., Landsverk, T., Schönheit, J., 1995b. Nephrotoxicity of *Narthecium ossifragum* in cattle in Norway. Vet. Rec. 137, 259–263.
Flåøyen, A., Bratberg, B., Frøslie, A., Grønstøl, H., Langseth, W., Mantle, P.G., von Krogh, A., 1997. Further studies on the presence, qualities and effects of the toxic princliples from *Narthecium ossifragum* plants. Vet. Res. Commun. 21, 137–148.
Fossen, T., Andersen, Ø.M., 2006. Spectroscopic techniques applied to flavonoids. In: Flavonoids: Chemistry, Biochemistry, and Applications. CRC Press, pp. 37–142.
Gaffield, W., Horowitz, R., Gentili, B., Chopin, J., Bouillant, M.L., 1978. Circular dichroism of C-glycosylflavones. A chiroptical method for differentiating 6-C, 8-C- and 6,8-di-C-β-glycosyl isomers. Tetrahedron 34, 3089–3096.
Harwig, J., Scott, P.M., 1971. Brine shrimp (*Artemia salina* L.) larvae as a screening system for fungal toxins. Appl. Microbiol. 21, 1011–1016.
Inoue, T., Mimaki, Y., Sashida, Y., Kobayashi, M., 1995. Structures of toxic steroidal saponins from *Narthecium asiaticum*. Chem. Pharm. Bull. 43, 1162–1166.
Jay, M., Ismaili, A., 1989. Flavones and *C*-glycosylflavones from the leaves of some *Arrhenatherum* species. Phytochemistry 28, 3035–3037.
Kobayashi, M., Suzuki, K., Nagasawa, S., Mimaki, Y., 1993. Purification of toxic saponins from *Narthecium asiaticum* Maxim. J. Vet. Med. Sci. 55, 401–407.
Li, Z., Gao, Y., Nakanishi, H., Gao, X., Cai, L., 2013. Biosynthesis of rare hexoses using microorganisms and related enzymes. Beilstein J. Org. Chem. 9, 2434–2445.
Matsuo, Y., MacLeod, R.A.F., Uphoff, C.C., Drexler, H.G., Nishizaki, C., Katayama, Y., Kimura, G., Fujii, N., Omoto, E., Harada, M., Orita, K., 1997. Two acute monocytic leukemia (AML-M5a) cell lines (MOLM-13 and MOLM-14) with interclonal phenotypic heterogeneity showing MLL-AF9 fusion resulting from an occult chromosome insertion, ins(11;9)(q23;p22p23). Leukemia 11, 1469–1477.
Melchert, T.E., Alston, R.E., 1965. Flavonoids from the moss *Mnium affine* Bland. Science 150, 1170–1171.
Meyer, B.N., Ferrighi, N.R., Putnam, J.E., Jacobsen, L.B., Nichols, D.E., McLaughlin, J.L., 1982. Brine shrimp: a convenient general bioassay for active plant constituents. Planta Med. 45, 31–34.
Miles, C., Munday, S., Holland, P.L.M., Wilkins, A., 1991. Identification of a sapogenin glucuronide in the bile of sheep affected by *Panicum dichoromiflorum* toxicosis. N. Z. Vet. J. 39, 150–152.
Mossberg, B., Stenberg, L., Ericsson, S., 1995. Gyldendals Store Nordiske Flora. GYLDENDAL NORSK FORLAG.
Mues, R., 1982. Flavone di-*C*-glycosides from the liverwort *Trichocolea tomentella* (L.) Dum. and their taxonomic significance. J. Hattori Bot. Lab. 51, 61–68.
Myhren, L., Mostrøm Nilssen, I., Nicolas, V., Døskeland, S.O., Barratt, G., Herfindal, L., 2014. Efficacy of multi-functional liposomes containing daunorubicin and emetine for treatment of acute myeloid leukaemia. Eur. J. Pharm. Biopharm. 88, 186–193.
Oftedal, L., Selheim, F., Wahlsten, M., Sivonen, K., Døskeland, S.O., Herfindal, L., 2010. Marine benthic cyanobacteria contain apoptosis-inducing activity synergizing with Daunorubicin to kill leukemia cells, but not cardiomyocytes. Mar. Drugs 8, 2659–2672.
Paulli, S., 1667. A Quadripartitum botanicum de simplicum medicamentorum. Argentorati: Impensis Fil. Simonis Paulli, pp. 690.
Pedersen, A.T., Andersen, Ø.M., Aksnes, D.W., Nerdal, W., 1995. Anomeric sugar configurations of anthocyanin *O*-pyranosides determined from heteronuclear one-bond coupling constants. Phytochem. Anal. 6, 313–316.
Quentmeier, H., Reinhardt, J., Zaborski, M., Drexler, H.G., 2003. FLT3 mutations in acute myeloid leukemia cell lines. Leukemia 17, 120–124.
Rayyan, S., Fossen, T., Nateland, H.S., Andersen, Ø.M., 2005. Isolation and identification of flavonoids, including flavone rotamers, from the herbal drug 'Crataegi Folium Cum Flore' (Hawthorn). Phytochem. Anal. 16, 334–341.
Sakakibara, M., Mabry, T.J., Bouillant, M.-L., Chopin, J., 1977. 6,8-di-*C*-glucosylflavones from *Larrea tridentate* (Zygophyllaceae). Phytochemistry 16, 1113–1114.
Salmenkallio, M., McCormick, S., Mabry, T.J., Dellamonica, G., Chopin, J., 1982. The flavonoids of *Trichophorum cespitosum*. Phytochemistry 21, 2990–2991.
Silva, B.M., Andrade, P.B., Ferreres, F., Seabra, R.M., Beatriz, M., Oliveira, P.P., Ferreira, M.A., 2005. Composition of Quince (*Cydonia oblonga* Miller) seeds: phenolics, organic acids and free amino acids. Nat. Prod. Res. 19, 275–281.
Stabursvik, A., 1953. A steroidal glycol, 22-Hydroxy-cholesterol from *Narthecium ossifragum* Huds. Acta Chem. Scand. 7 1220–1220.
Stabursvik, A., 1959. A Phytochemical Study of Narthecium Ossifragum (L.) Huds. Doctoral thesis NTH. Technical University of Norway, Trondheim.
Sy, L.K., Lok, C.N., Wang, J.Y., Liu, Y., Cheng, L., Wan, P.K., Leung, C.T., Cao, B., Kwong, W.L., Chang, R.C.C., Che, C.M., 2016. Identification of "sarsapogenin-aglyconed" timosaponins as novel Abeta-lowering modulators of amyloid precursor protein processing. Royal Soc. Chem. 7, 3206–3214.
Tønnesen, H.H., Mysterud, I., Karlsen, J., Skulberg, O.M., Laane, C.M.M., Schumacher, T., 2013. Identification of singlet oxygen photosensitizes in lambs drinking water in an alveld risk area in West Norway. J. Photochem. Photobiol. B Biol. 119, 37–45.
Uhlig, S., Wisløff, H., Petersen, D., 2007. Identification of cytotoxic constituents of *Narthecium ossifragum* using bioassay-guided fractionation. J. Agric. Food Chem. 55, 6018–6026.
Viktorsson, E.Ö., Grøthe, B.M., Aesoy, R., Sabir, M., Snellingen, S., Prandina, A., Åstrand, O.A.H., Bonge-Hansen, T., Døskeland, S.O., Herfindal, L., Rongved, P., 2017. Total synthesis and antileukemic evaluations of the phenazine 5,10-dioxide natural products iodinin, myxin and their derivatives. Bioorg. Med. Chem. 25, 2285–2293.
Vu, M., Herfindal, L., Juvik, O.J., Vedeler, A., Haavik, S., Fossen, T., 2016. Toxic aromatic compounds from fruits of *Narthecium ossifragum* L. Phytochemistry 132, 76–85.
Wellman, K., Laur, P.H.A., Briggs, W.S., Moscowitz, A., Djerassi, C., 1965. Optical Rotatory Dispersion Studies. XCIX. Superposed multiple cotton effects of saturated ketones and their significance in the circular dichroism measurement of (-)-menthone. J. Am. Chem. Soc. 87, 66–72.
Wisløff, H., Flåøyen, A., Ottesen, N., Hovig, T., 2003. *Narthecium ossifragum* (L.) Huds. Causes kidney damage in goats: morphologic and functional effects. Vet. Pathol. 40, 317–327.
Wu, C., 2014. An important player in brine shrimp lethality bioassay: the solvent. "J. Adv. Pharm. Technol. Research"" (JAPTR)" 5, 57–58.